Atmos. Meas. Tech. Discuss., doi:10.5194/amt-2016-390, 2017
Manuscript under review for journal Atmos. Meas. Tech.
Published: 6 February 2017

Atmospheric Measurement Techniques Discussions

Development and validation of a CCD-laser aerosol detective system for measuring the ambient aerosol phase function

Yuxuan Bian[1,2], Chunsheng Zhao[2], Wanyun Xu[3], Gang Zhao[2], Jiangchuan Tao[2], Ye Kuang[2]

[1]State Key Laboratory of Severe Weather, Chinese Academy of Meteorological Sciences, Beijing, 100081, China
[2]Department of Atmospheric and Oceanic Sciences, School of Physics, Peking University, Beijing, 100871, China
[3]State Key Laboratory of Severe Weather & Key Laboratory of Atmospheric Chemistry of CMA, Chinese Academy of Meteorological Sciences, Beijing, 100081, China

Correspondence to: Chunsheng Zhao (zcs@pku.edu.cn)

Abstract. Aerosol phase function represents the angular scattering property of aerosols, which is crucial for understanding the climate effects of aerosols that have been identified as one of the largest uncertainties in the evaluation of radiative forcing. So far, there is a lack of instruments to measure the aerosol phase function directly and accurately in laboratory studies and in-situ measurements. A portable instrument with high angular range and resolution has been developed for the measurement of the phase function of ambient aerosols in this study. The charge-coupled device-laser aerosol detective system (CCD-LADS), which measures the aerosol phase function both across a relatively wide angular range of 10 °-170 °and at a high resolution of 0.1 °. The system includes a continuous laser, two charge-coupled device cameras and the corresponding fisheye lenses. The CCD-LADS was validated by both a laboratory study and a field measurement. The comparison between the aerosol phase function retrieved from CCD-LADS and Mie-scattering model shows good agreement. Compared with the TSI polar nephelometer, CCD-LADS has the advantages of wider detection range and better stability.

1 Introduction

The climate effect of aerosol optical properties is one of the greatest uncertainties in our understanding about the climate change. Instruments such as the integrating nephelometer were often used to measure the aerosol scattering coefficient in laboratory studies and field campaigns (Ma et al., 2011; Tao et al., 2014). However, besides the total scattering coefficient, the distribution of aerosol scattering at different directions also has significant impact on the direct climate effect of aerosols (Kuang et al., 2015; Kuang et al., 2016b). The Aerosol phase function ($p(\theta)$) is defined to describe the angular distribution of the aerosol scattering intensity. If the particle is assumed to be spherical, there is a comprehensive theory named the Mie scattering theory to describe the characteristics of aerosol scattering, when the particle size is in the same scale with the wavelength of scattering light. $p(\theta)$ can also be calculated with the size and complex refractive index of particles by the Mie theory (Kim et al., 2010). In past years, different research groups have developed several versions of polar nephelometers to measure how the scattering intensities of aerosol particles, cloud droplets and ice crystals changes with scattering angle. Muñoz et al. (2001, 2010, 2011) mounted a photomultiplier tube (PMT) on a mechanical arm which can rotate around a point on the

Atmos. Meas. Tech. Discuss., doi:10.5194/amt-2016-390, 2017
Manuscript under review for journal Atmos. Meas. Tech.
Published: 6 February 2017

Atmospheric Measurement Techniques Discussions

laser light path in the same plane with the laser beam to change the scattering angle of the signal captured by the PMT. Barkey et al. (2002, 2007) made the sample flow perpendicular and intersect with the light path. Then many PMTs were mounted around the point of intersection in the same plane with the laser beam to capture the scattering signal from different scattering angles. Castagner and Bigio (2006, 2007) focused the light scattered at a single spot with different scattering angles to another single spot by using two parabolic reflectors next to the light path. A plane mirror was settled at that point and reflect the scattering signals with different angles to a PMT by rotation. Curtis et al. (2007,2008) used an ellipsoidal mirror to reflect the scattering light to a linearity charge-coupled device (CCD) detector for the detection of aerosol phase function. This method can offer a better angle and time resolution at a wider range of scattering angles than the other methods above. It just needs one detector and there is no need to move the detector during the measurement.

Recently, McCrowey et al. (2013) developed a miniaturized polar nephelometer, which can be used in the in-situ measurement based on the techniques of Curtis et al. (2007) and can then be calibrated in the laboratory using polystyrene latex (PSL) standard particles. A comparison between the results measured from this instrument and calculated from a Mie model showed a good agreement. The detection range of this instrument is from 20 to 155 °scattering angle. Besides these studies, the Aurora 4000 polar nephelometer (Ecotech Pty Ltd., Australia) is currently the only commercial instrument that can measure the aerosol phase function. This product has a structure similar to that of the integrating nephelometer, while a backscatter shutter that is able to be positioned at any angle between 10-90 ° is mounted in the cavity to help the nephelometer measuring the light scattering from that angle, through to 170 °. The Aurora 4000 can just measure the aerosol phase function in a scattering angle range of 0-90 °for dry aerosols.

A novel instrument named charge-coupled device-laser aerosol detective system (CCD-LADS) based on the CCD imaging principle and the optical structure of the fisheye lens is developed to measure the ambient aerosol phase function in the field measurement at a wider range of detection angles and a higher accuracy. The validation in both laboratory and field measurement shows the ability of the CCD-LADS to measure the aerosol phase function.

2 Instrumentation and Methodology

2.1 Design of instrument

The CCD-LADS includes several main components: a high power continuous laser emitter, two CCD cameras, optical filters and fisheye lenses. The laser and CCD cameras are mounted on tripods and controlled by a laptop. Each component is portable and on a scale of a few cubic decimeters.

The emitting system of the CCD-LADS is mainly built with a solid continuous laser emitter. Nd: YAG is used as the solid laser material as the wavelength of the emitter is 532 nm. The power of the laser is 1 W.

Atmos. Meas. Tech. Discuss., doi:10.5194/amt-2016-390, 2017
Manuscript under review for journal Atmos. Meas. Tech.
Published: 6 February 2017

The receiving system of CCD-LADS has three main parts, the CCD cameras, the optical filters and the fisheye lenses. The SBIG model STF-8300 CCD imaging camera, which has the KAF-8300 CCD sensor (ON Semiconductor, Phoenix, AZ, USA) is used. The area array (17.96*13.52 mm) of pixels has 8.3 million (3326*2504) effective pixels, while each pixel is a square 5.4 μm on a side. The exposure time is from 0.1s to 1h. Due to its outstanding performance, this product is often used in astronomical measurements and also measurements in the other research areas (Coenen et al., 2015).

The fisheye lens (Sigma Corp., Japan) has a 10 mm focus length and a F2.8 aperture. When this lens is used with a Nikon camera, the field of view can be 180 °. Because of the size of the CCD arrays, when this lens is used with the STF-8300 camera, the field of view is about 120 °. The equisolid projection, which means that the solid angle of the object is directly proportional to the area on the CCD arrays, is used by this lens (Miyamoto, 1964).

To filter out the background noise from the sky radiation, an optical filter (Thorlabs, Newton, NJ, USA) is mounted between the CCD camera and the lens. The filter has a 532 ±2 nm wavelength, and a 10 ±2 nm full width at half maximum, while the minimum transmission at the peak is 70%.

Figure 1 is the sketch map of the geometric relationship of CCD-LADS. The laser is emitted horizontally, while a light trap is used to receive the laser beam on the other side. Besides the laser beam, two CCD cameras with fisheye lenses are installed at the same altitude with the laser to capture the scattering signal from the laser beam, while the directions of the cameras are forward and backward, respectively. When two CCD cameras are used in this system, the detective angle can be expanded to 160 ° from 10-170 °. The angle resolution can reach 0.1 ° per pixel. The scattering signal from 0-10 ° and 170-180 ° cannot be detected, because the signal to noise ratio is significantly lower than the value needed to estimate the quantities effectively.

To decrease the total area of the instrument, the distance between the CCD cameras and the laser beam should be less than 1m. So the whole CCD-LADS system should cover an area of 12m long and 1m wide. When the instrument is set up, the first step to do is to measure the relative position of the CCD cameras, the laser beam and the laser emitter. From the geometric relationship shown in figure 1, we can know that the light scattered at different position on the laser beam will be collected by different pixels on the CCD, so that the scattering light at different angles can be retrieved from the image captured by CCD. Due to the open path structure of the CCD-LADS, the background noise is much higher in daytime than in nighttime.

2.2 Methodology

2.2.1 Data acquisition and pre-processing

The data acquisition of CCD-LADS is to merge the signals captured from two independent CCD system, which can detect the scattering light from different scattering angles. The exposure time of these two CCDs should be in complete accord for the comparison.

At the beginning of the measurement, a dark frame image is captured for each CCD by using a shutter in front of the lens. The bias noise from the process and transmission of the signal can be subtracted during the procedure of image configuration by

Atmos. Meas. Tech. Discuss., doi:10.5194/amt-2016-390, 2017
Manuscript under review for journal Atmos. Meas. Tech.
Published: 6 February 2017

Atmospheric Measurement Techniques Discussions

subtracting the dark frame image from the regular image. Then a suitable exposure time is set to measure the scattering light. After image capture, the central axis of the signals from the scattering light is fitted in the program. Then the signal intensity of the scattering light from different scattering angle is analysed to get the angle-resolved signal.

When the angle-resolved signals from two CCDs are retrieved, the change of signals with angles can be merged. Firstly, the transform coefficient with scattering angles $\mathrm{T}(\theta)$ is calculated by using the overlap region of signals from two CCDs after quality control,

$$\mathrm{T}(\theta) = \frac{I_1(\theta)}{I_2(\theta)} \quad (1)$$

$I_1(\theta)$ is the signal captured by the first CCD while $I_2(\theta)$ is that of the second CCD. The transform coefficient T is an average of $\mathrm{T}(\theta)$. The signal $I_2'(\theta)$ can be calculated by multiplying $I_2(\theta)$ with T. For the region of scattering angles that just one CCD can captured, the signal $I_1(\theta)$ or $I_2'(\theta)$ is used as the scattering signals after merging. For the overlap region, a linear weighting average is done between $I_1(\theta)$ and $I_2'(\theta)$. If the scattering angle is closer to the angle that just $I_1(\theta)$ can represent, the share of $I_1(\theta)$ is higher than $I_2'(\theta)$ and vice versa. Using the method above, the merged signals with scattering angles can be estimated.

2.2.2 The retrieval algorithm to determine aerosol phase function

Figure 2 shows the flow chart of the retrieval algorithm to determine $\mathrm{p}(\theta)$ from CCD-LADS measurements. According to the geometric structure of the CCD-LADS, the echo equation of CCD-LADS can be figured firstly,

$$\mathrm{E}(\theta) = \mathrm{N}_0\tau_Z\tau_R\beta(\theta) \quad (2)$$

where $\mathrm{E}(\theta)$ is the received signals with scattering angles, $\beta(\theta)$ is the scattering function of atmospheric air molecules and aerosols, τ_Z and τ_R are the transmittances on the optical paths of laser emitting and scattering respectively, N_0 is the transform coefficient of the instrument. The longest distance between CCD cameras and the points on the laser beam is limited to less than 10m in the scattering range from 10 °to 170 °. In this range, an assumption that $\tau_Z = \tau_R = 1$ can be established and equation (2) can be transformed to $\mathrm{E}(\theta) = \mathrm{N}_0\beta(\theta)$.

Aerosol phase function $\mathrm{p}(\theta)$ is the normalized angular distribution of the scattering function. If the scattering function of aerosols $\beta_{aero}(\theta)$ is known, the $\mathrm{p}(\theta)$ can be calculated. Therefore, a retrieval algorithm is built to separate the scattering signals with angles into the scattering of aerosols and air molecules.

As the first step, the scattering coefficient of air molecules at near surface level k_{sc-air} is calculated with the density of atmosphere, which depends on the surface pressure and temperature,

$$\mathrm{k}_{sc-air} = \frac{8\pi^3(m^2-1)^2}{3n_{air}\lambda^4} \quad (3)$$

where n_{air} is the number density of air molecules, m is the index of refraction of atmosphere, which depends on n_{air} and the wavelength of the laser λ. The hemispheric backscattering coefficient of air molecules $\mathrm{k}_{bsc-air}$ is a half of k_{sc-air}.

Atmos. Meas. Tech. Discuss., doi:10.5194/amt-2016-390, 2017
Manuscript under review for journal Atmos. Meas. Tech.
Published: 6 February 2017

Atmospheric Measurement Techniques Discussions

To resolve the ratio between the air and aerosol scattering, the scattering coefficient of aerosols $k_{sc-aero}$ and the hemispheric backscattering coefficient of aerosols $k_{bsc-aero}$ are measured with an intergrating nephelometer here.

The normalized parameter of air molecules scatter N_1 and N_2 can be calculated with k_{sc-air}, $k_{sc-aero}$, $k_{bsc-air}$ and $k_{bsc-aero}$,

$$N_1 = \frac{\int_0^{2\pi}\int_0^{\pi} E(\theta)\sin\theta d\theta d\varphi \times \frac{k_{sc-air}}{k_{sc-air}+k_{sc-aero}}}{4\pi} \quad (4)$$

$$N_2 = \frac{\int_0^{2\pi}\int_{\pi/2}^{\pi} E(\theta)\sin\theta d\theta d\varphi \times \frac{k_{bsc-air}}{k_{bsc-air}+k_{bsc-aero}}}{2\pi} \quad (5)$$

where N_1 and N_2 are calculated with the total scattering coefficient and the hemispheric backscattering coefficient separately. The received scattering signals are integrated on the spherical surface, and then multiplied by the percentage of air scattering to get these parameters. The physical significance of these parameters is to indicate the intensity of air scatter.

Because of the detective angular range of CCD-LADS is 10-170 degree, the angular truncation correction is necessary to resolve the total scattering intensity. For the forward angular truncation, several aerosol phase functions proposed in the previous studies are used to calculate the correlation coefficient with the signal profile, and then the one with a best correlation is chosen to fit the signal profile in this angular range. For the backward angular truncation, the scattering intensity in that range is assumed to be equal to the scattering intensity at the largest scattering angle that CCD-LADS can measured. After the correction above, the corrected intensity $E'(\theta)$ is used in equation (4) and (5) to resolve the N_1 and N_2.

If the difference between N_1 and N_2 is less than 10% in the test, the result will be accepted. Combine the normalized parameter, air scattering phase function and $E'(\theta)$, the scattering intensities of aerosols with scattering angles ($E_{aero}(\theta)$) can be calculated,

$$E_{aero}(\theta) = E'(\theta) - \frac{3(1+\cos^2\theta)}{4} \times \frac{N_1+N_2}{2} \quad (6)$$

Because the $p(\theta)$ is a normalized function and directly proportional to $E_{aero}(\theta)$, it can be normalized with $E_{aero}(\theta)$.

3 Results

3.1 Laboratory Results

To validate the ability of the CCD-LADS to measure the aerosol phase function, an indoor experiment was held in the laboratory in the Physics Building at Peking University during November 7-8th, 2015. The time resolution of CCD-LADS was set to 60 s during the experiment, while the angular detection ranged from 10 to 170 °. The aerosol scattering coefficient, number size distribution, mass concentration of black carbon particles, ambient temperature and relative humidity were measured with an integrating nephelometer (Model 3563, TSI, Inc., Shoreview, MN, USA), a scanned mobility particle sizer (Model 3936, TSI, Inc., Shoreview, MN, USA), an aerodynamic particle sizer (Model 3321, TSI, Inc., Shoreview, MN, USA),

Atmos. Meas. Tech. Discuss., doi:10.5194/amt-2016-390, 2017
Manuscript under review for journal Atmos. Meas. Tech.
Published: 6 February 2017

Atmospheric Measurement Techniques Discussions

a micro-aethalometer (Model AE51, Magee Scientific, Berkeley, CA, USA) and a dew-point chilled mirror sensor (Edgetech DewMaster), respectively.

Figure 3 shows the time series of several quantities during the laboratory experiment. The scattering/hemispheric backscattering coefficient of aerosols at 525nm wavelength shown in fig. 3(b) and the mass concentration of black carbon particles shown in fig. 3(c) reveal the same pattern that first declines and climbs up afterwards. The same pattern can be discovered in the time series of particle number size distributions shown in fig. 3(d). The variation reflects the slow exchange between the air indoor and outdoor. The peak diameter of aerosol number size distribution was still around 100nm, while it had a slight shift during the experiment. Therefore, the fine particles are dominant in the laboratory. The single scattering albedo (SSA) shown in fig. 3(c) was around 0.85 which means that the black carbon aerosol took up a relatively large proportion among the aerosol species, resulting in strong particle light absorption ability.

Combining the particle number size distributions and the mass concentration of black carbon aerosols into a modified Mie-scattering model, the aerosol optical properties including the aerosol phase function could be modelled (Ma et al., 2011). In this study, the ratio between two different mixing states (external or core-shell) of black carbon aerosols is assumed to be 1:1 according to the result of Ma et al. (2012). Figure 4 shows the comparison among the aerosol phase functions retrieved with the CCD-LADS retrieval algorithm, modelled with the modified Mie model and offered by the aerosol classification from the Cloud-Aerosol Lidar and Infrared Pathfinder Satellite Observations (CALIPSO) aerosol products (Omar et al., 2009). Here the red solid line shows the retrieved $\mathrm{p}(\theta)$ from the CCD-LADS measurements with the retrieval algorithm introduced in Sect. 2.2.2, while the brown dashed line shows the retrieved $\mathrm{p}(\theta)$ from CCD-LADS directly without considering the air molecules scattering influence. The blue dashed line shows the modelled result, and the other dotted lines express the aerosol phase functions of different aerosol types from CALIPSO aerosol classification. The result shows that the comparison between the modelled $\mathrm{p}(\theta)$ and the $\mathrm{p}(\theta)$ retrieved with the retrieval algorithm shows a better agreement than the comparison between the modelled $\mathrm{p}(\theta)$ and the $\mathrm{p}(\theta)$ retrieved from the CCD-LADS measurements directly, especially for the backward scattering. The reason of this phenomenon is that the scattering abilities of aerosols and air molecules are closer to each other for the backward scatter than for the forward scatter. The comparison also shows that the retrieved $\mathrm{p}(\theta)$ is closer to the aerosol phase function of the "biomass burning" aerosol among the several aerosol types classified from CALIPSO aerosol products. Compared with the other aerosol types, the "biomass burning" aerosol represents a better absorption ability due to the larger percentage of black carbon aerosol, and also a smaller effective diameter which is lower than 100nm. The SSA and particle number size distribution of aerosols during the experiment shown in fig. 3 also have the similar characteristics with the "biomass burning" aerosol.

To further validate the quality of the retrieved result from the CCD-LADS measurement, a comparison was also carried out among the $\mathrm{p}(\theta)$ at 42 degree scattering angle resolved with different methods (figure 5). The $\mathrm{p}(\theta)$ at 42 degree scattering angle is relatively typical and comparable because 42 degree is the scattering angle used in the forward scattering visibility

Atmos. Meas. Tech. Discuss., doi:10.5194/amt-2016-390, 2017
Manuscript under review for journal Atmos. Meas. Tech.
Published: 6 February 2017

Atmospheric Measurement Techniques Discussions

sensor (Kessner et al., 2013). The result of the comparison shows that the $p(\theta)$ from CCD-LADS measurement and Mie model have the same pattern and the difference in the absolute values between these two $p(\theta)$ is not obvious.

3.2 Field Measurements

During January 2016, a comprehensive field campaign focused on air pollution in winter was conducted at the roof of a school building in Yanqi campus of the University of Chinese Academy of sciences (UCAS) in Huairou district, Beijing (40°24′ N, 116°40′ E, 91 m a.s.l.). The observatory is 60 km away from the downtown of Beijing and is at the edge of the North China Plain (NCP), which makes it suitable for measuring the regional pollution properties of the NCP (Ma et al., 2016). During the campaign, all the instruments except for the CCD-LADS were housed in a laboratory with a steady room temperature as 20 ℃. The aerosols were sampled from an inlet 5 m higher than the ground and then dried to a relative humidity less than 30% before flowing into the laboratory to measure the aerosol number size distribution, scattering coefficient, phase function and the mass concentration of black carbon aerosols at a dry condition. The CCD-LADS was mounted outside the laboratory at the same altitude to measure the scattering phase function of ambient aerosols. Depending on the limitation of the ambient condition, the angular detection range of the CCD-LADS was 30-160 °in this campaign.

During the field measurement, the scattering phase function of dry aerosols could be resolved from two ways: Aurora 4000 polar nephelometer measurements and the modified Mie-scattering model with the related aerosol measurements. Under high relative humidity condition, aerosol particles will absorb moisture in the atmosphere and grow up significantly (Bian et al., 2014; Chen et al., 2014; Kuang et al., 2016a), and hence the scattering properties of ambient and dry aerosols are totally different. Therefore, the data collected at a relative humidity above 70% were kicked off from the comparison among the scattering phase functions of dry and ambient aerosols obtained by different methods. Figure 6 shows the result of the comparison mentioned above. The results from three methods are consistent with one another in the overlap of the detectable scattering angular range. Compared with the other results, the retrieval of CCD-LADS measurement enhances the backward scattering fraction of aerosol. This might be caused by the angular range (30-160 °), which did not reach 10-170 °and therefore might have increased errors in retrieving the angular distribution of aerosol scattering. The $p(\theta)$ from Aurora 4000 measurements have the similar average pattern with the results from other methods, but the deviation of its pattern is also obvious. Compared to the Aurora 4000 results, there are two significant advantages of CCD-LADS: wider detection range and better stability.

4 Discussions and Conclusions

A novel instrument named charge-coupled device-laser aerosol detective system (CCD-LADS) was developed to measure the ambient aerosol phase function in the ambient atmosphere at a wider range of detection angles and a higher accuracy. The validation in both laboratory and field measurement shows the ability of CCD-LADS to measure the aerosol phase function.

Atmos. Meas. Tech. Discuss., doi:10.5194/amt-2016-390, 2017
Manuscript under review for journal Atmos. Meas. Tech.
Published: 6 February 2017

Atmospheric Measurement Techniques Discussions

A laser is emitted horizontally, while two CCD cameras with fisheye lenses are installed besides the laser beam at the same altitude to capture the scattering signal from the laser beam with the cameras facing forward and backward, respectively. Then the signal captured by the two cameras are merged into one signal curve. The detectable angular range is from 10-170 °, while the angle resolution reach 0.1 °per pixel. A retrieval algorithm is developed to subtract the influence of air molecules scattering with the integrating nephelometer and weather station measurements.

To validate the ability of CCD-LADS to measure the aerosol phase function, an indoor experiment was held in the laboratory of the Physics Building at Peking University during November 7-8th, 2015. During the experiment, the angular detection range was from 10-170 °. The comparison between the modelled $p(\theta)$ and the retrieved $p(\theta)$ shows an excellent agreement. Both of them are close to the aerosol phase function of the "biomass burning" aerosol from CALIPSO aerosol products. The comparison result is reasonable, because the SSA and particle number size distribution of aerosols during the experiment also had similar characteristics with the "biomass burning" aerosol. The comparison of the $p(\theta)$ at 42 °scattering angle acquired by different methods also shows good agreements on both patterns and absolute values.

During January 2016, a comprehensive field campaign focused on air pollution in winter was organized at the roof of a school building in Yanqi campus of the UCAS. Depending on the limitation of ambient condition, the angular detection range of the CCD-LADS was 30-160 °in this campaign. The retrieved aerosol phase function with CCD-LADS measurements is consistent with both the Aurora 4000 measurement and the modified Mie model results in the overlap region of the detectable scattering angular range. Compared with the Aurora 4000 measurements during this campaign, the CCD-LADS measurements are steadier.

Both the laboratory experiment and the field measurement have demonstrated that the CCD-LADS is a robust instrument, fully capable of measuring the ambient aerosol phase function under different conditions. Overall, compared with the laboratory-scale instruments, the CCD-LADS measured aerosol phase functions in a wider angular range and a higher angular resolution.

Acknowledgements

This work is supported by the National Natural Science Foundation of China (41590872, 41375134).

References

Barkey, B., Bailey, M., Liou, K.-N., and Hallett, J.: Light-scattering properties of plate and column ice crystals generated in a laboratory cold chamber, Applied Optics, 41, 5792-5796, 2002.

Barkey, B., Paulson, S. E., and Chung, A.: Genetic Algorithm Inversion of Dual Polarization Polar Nephelometer Data to Determine Aerosol Refractive Index, Aerosol Science and Technology, 41, 751-760, 2007.

Bian, Y. X., Zhao, C. S., Ma, N., Chen, J., and Xu, W. Y.: A study of aerosol liquid water content based on hygroscopicity measurements at high relative humidity in the North China Plain, Atmos. Chem. Phys., 14, 6417-6426, 2014.

Castagner, J.-L. and Bigio, I. J.: Particle sizing with a fast polar nephelometer, Applied Optics, 46, 527-532, 2007.

Castagner, J.-L. and Bigio, I. J.: Polar nephelometer based on a rotational confocal imaging setup, Applied Optics, 45, 2232-2239, 2006.

Chen, J., Zhao, C. S., Ma, N., and Yan, P.: Aerosol hygroscopicity parameter derived from the light scattering enhancement factor measurements in the North China Plain, Atmos. Chem. Phys., 14, 8105-8118, 2014.

Curtis, D. B., Aycibin, M., Young, M. A., Grassian, V. H., and Kleiber, P. D.: Simultaneous measurement of light-scattering properties and particle size distribution for aerosols: Application to ammonium sulfate and quartz aerosol particles, Atmospheric Environment, 41, 4748-4758, 2007.

Curtis, D. B., Meland, B., Aycibin, M., Arnold, N. P., Grassian, V. H., Young, M. A., and Kleiber, P. D.: A laboratory investigation of light scattering from representative components of mineral dust aerosol at a wavelength of 550 nm, Journal of Geophysical Research: Atmospheres, 113, D08210, 2008.

Draine, B. T. and Flatau, P. J.: Discrete-Dipole Approximation For Scattering Calculations, Journal of the Optical Society of America A, 11, 1491-1499, 1994.

Kessner, A. L., Wang, J., Levy, R. C., and Colarco, P. R.: Remote sensing of surface visibility from space: A look at the United States East Coast, Atmospheric Environment, 81, 136-147, 2013.

Kim, H., Barkey, B., and Paulson, S. E.: Real refractive indices of α- and β-pinene and toluene secondary organic aerosols generated from ozonolysis and photo-oxidation, Journal of Geophysical Research: Atmospheres, 115, D24212, 2010.

Kuang, Y., Zhao, C. S., Ma, N., Liu, H. J., Bian, Y. X., Tao, J. C., and Hu, M.: Deliquescent phenomena of ambient aerosols on the North China Plain, Geophysical Research Letters, 43, 8744-8750, 2016a.

Kuang, Y., Zhao, C. S., Tao, J. C., Bian, Y. X., and Ma, N.: Impact of aerosol hygroscopic growth on the direct aerosol radiative effect in summer on North China Plain, Atmospheric Environment, 147, 224-233, 2016b.

Kuang, Y., Zhao, C. S., Tao, J. C., and Ma, N.: Diurnal variations of aerosol optical properties in the North China Plain and their influences on the estimates of direct aerosol radiative effect, Atmos. Chem. Phys., 15, 5761-5772, 2015.

Ma, N., Zhao, C., Tao, J., Wu, Z., Kecorius, S., Wang, Z., Größ, J., Liu, H., Bian, Y., Kuang, Y., Teich, M., Spindler, G., Müller, K., van Pinxteren, D., Herrmann, H., Hu, M., and Wiedensohler, A.: Variation of CCN activity during new particle formation events in the North China Plain, Atmos. Chem. Phys., 16, 8593-8607, 2016.

Ma, N., Zhao, C. S., Müller, T., Cheng, Y. F., Liu, P. F., Deng, Z. Z., Xu, W. Y., Ran, L., Nekat, B., van Pinxteren, D., Gnauk, T., Müller, K., Herrmann, H., Yan, P., Zhou, X. J., and Wiedensohler, A.: A new method to determine the mixing state of light absorbing carbonaceous using the measured aerosol optical properties and number size distributions, Atmos. Chem. Phys., 12, 2381-2397, 2012.

Ma, N., Zhao, C. S., Nowak, A., Müller, T., Pfeifer, S., Cheng, Y. F., Deng, Z. Z., Liu, P. F., Xu, W. Y., Ran, L., Yan, P., Göbel, T., Hallbauer, E., Mildenberger, K., Henning, S., Yu, J., Chen, L. L., Zhou, X. J., Stratmann, F., and Wiedensohler, A.: Aerosol optical properties in the North China Plain during HaChi campaign: an in-situ optical closure study, Atmos. Chem. Phys., 11, 5959-5973, 2011.

McCrowey, C. J., Tinilau, S. S., Calderon, G., Koo, J.-E., and Curtis, D. B.: A Portable High-Resolution Polar Nephelometer for Measurement of the Angular Scattering Properties of Atmospheric Aerosol: Design and Validation, Aerosol Science and Technology, 47, 592-605, 2013.

Mishchenko, M. I., Travis, L. D., and Mackowski, D. W.: T-matrix computations of light scattering by nonspherical particles: A review, Journal of Quantitative Spectroscopy and Radiative Transfer, 55, 535-575, 1996.

Muñoz, O. and Hovenier, J. W.: Laboratory measurements of single light scattering by ensembles of randomly oriented small irregular particles in air. A review, Journal of Quantitative Spectroscopy and Radiative Transfer, 112, 1646-1657, 2011.

Muñoz, O., Moreno, F., Guirado, D., Ramos, J. L., López, A., Girela, F., Jerónimo, J. M., Costillo, L. P., and Bustamante, I.: Experimental determination of scattering matrices of dust particles at visible wavelengths: The IAA light scattering apparatus, Journal of Quantitative Spectroscopy and Radiative Transfer, 111, 187-196, 2010.

Muñoz, O., Volten, H., de Haan, J. F., Vassen, W., and Hovenier, J. W.: Experimental determination of scattering matrices of randomly oriented fly ash and clay particles at 442 and 633 nm, Journal of Geophysical Research: Atmospheres, 106, 22833-22844, 2001.

Omar, A. H., Winker, D. M., Vaughan, M. A., Hu, Y., Trepte, C. R., Ferrare, R. A., Lee, K.-P., Hostetler, C. A., Kittaka, C., Rogers, R. R., Kuehn, R. E., and Liu, Z.: The CALIPSO Automated Aerosol Classification and Lidar Ratio Selection Algorithm, Journal of Atmospheric and Oceanic Technology, 26, 1994-2014, 2009.

Tao, J. C., Zhao, C. S., Ma, N., and Liu, P. F.: The impact of aerosol hygroscopic growth on the single-scattering albedo and its application on the NO2 photolysis rate coefficient, Atmos. Chem. Phys., 14, 12055-12067, 2014.

Atmos. Meas. Tech. Discuss., doi:10.5194/amt-2016-390, 2017
Manuscript under review for journal Atmos. Meas. Tech.
Published: 6 February 2017

Atmospheric Measurement Techniques Discussions

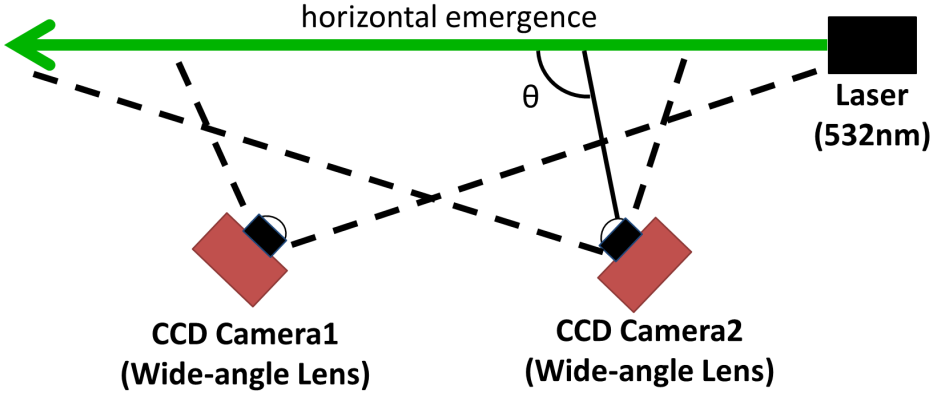

Figure 1: Sketch map of the geometric relationship of CCD-LADS

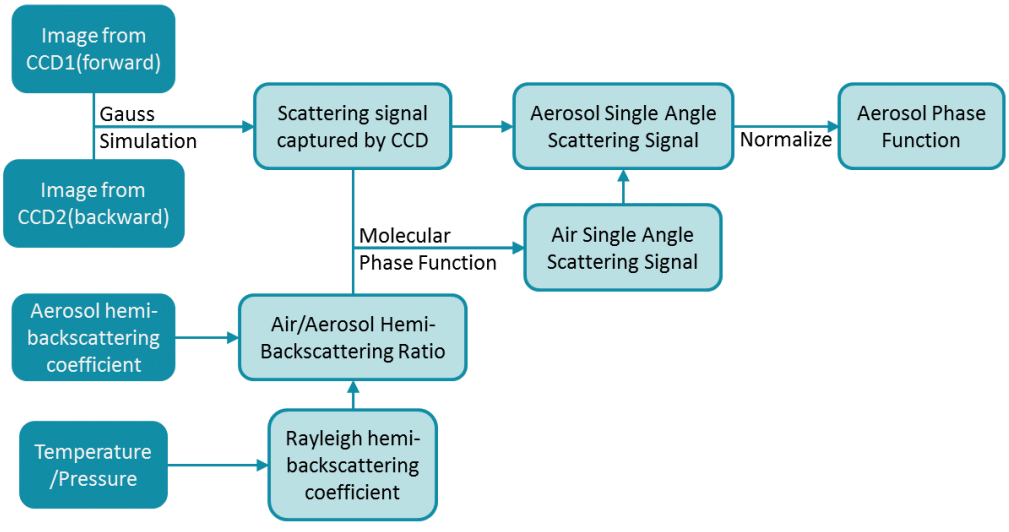

Figure 2: Flow chart of the retrieval algorithm to determine aerosol phase function from CCD-LADS measurements

Atmos. Meas. Tech. Discuss., doi:10.5194/amt-2016-390, 2017
Manuscript under review for journal Atmos. Meas. Tech.
Published: 6 February 2017

Atmospheric Measurement Techniques Discussions

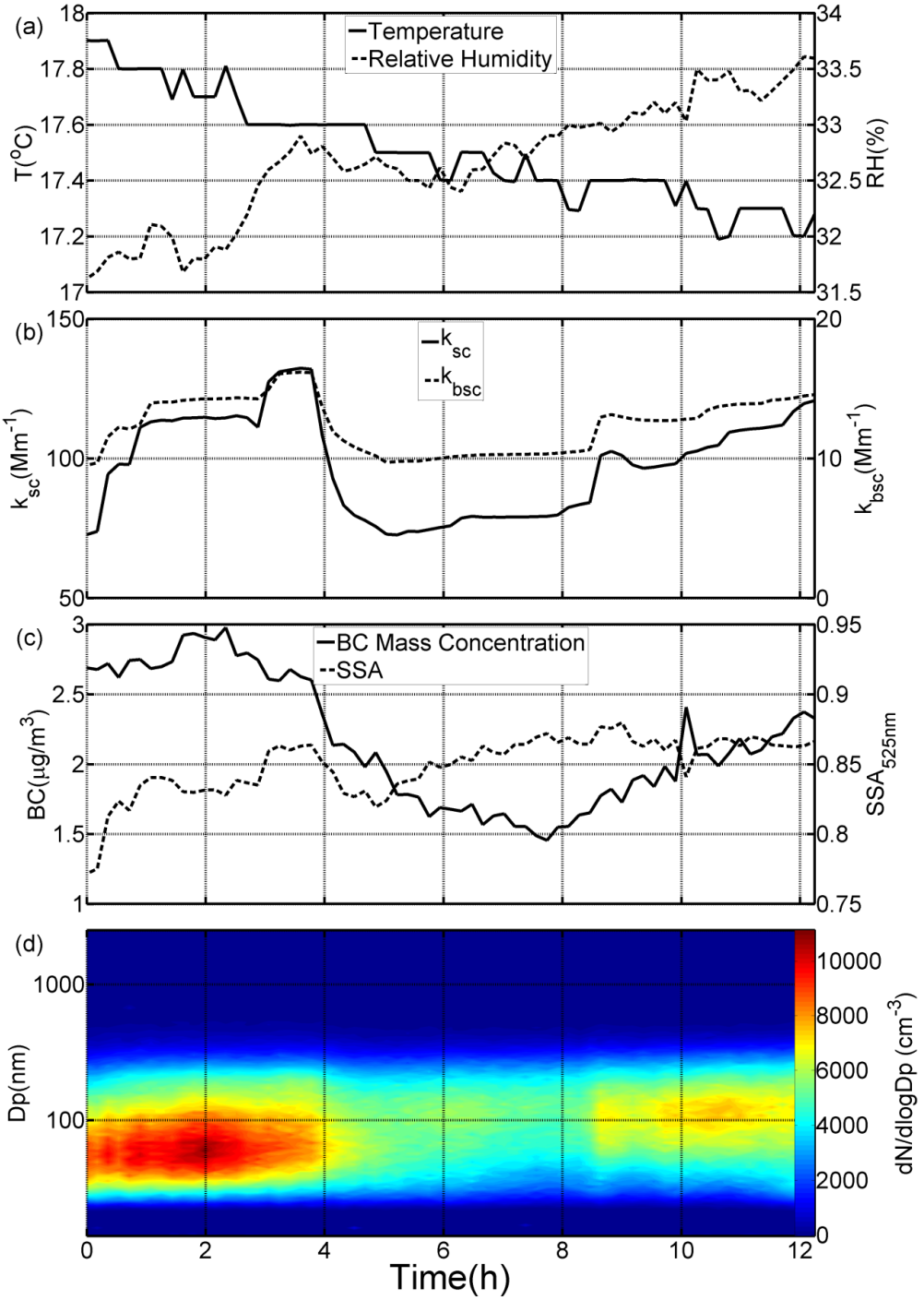

Figure 3: Time series (a) temperature (solid line) and relative humidity (dashed line) in the laboratory, (b) scattering coefficient (solid line) and hemispheric backscattering coefficient (dashed line) of aerosols at 525nm wavelength, (c) mass concentration of black carbon particles (solid line) and single scattering albedo of aerosols at 525nm wavelength (dashed line), (d) PNSD of aerosols during the laboratory study at Peking University in 2015.

Atmos. Meas. Tech. Discuss., doi:10.5194/amt-2016-390, 2017
Manuscript under review for journal Atmos. Meas. Tech.
Published: 6 February 2017

Atmospheric Measurement Techniques Discussions

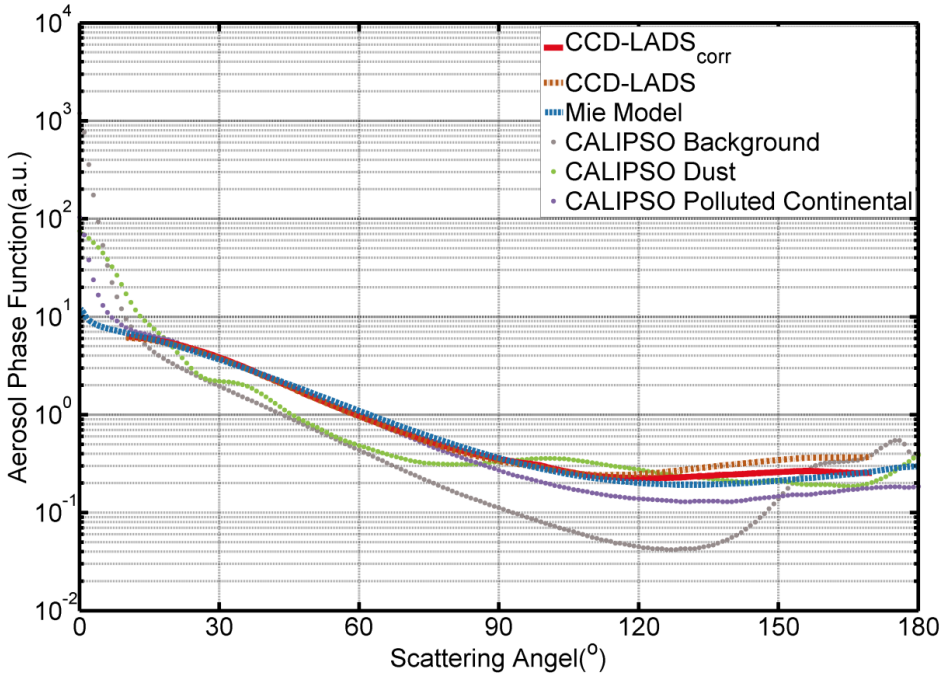

Figure 4: Comparison between aerosol phase function obtained from CCD-LADS measurements (red solid line shows the result estimated with the retrieval algorithm, brown dashed line shows that estimated directly with the measurements), modelled with modified Mie model (blue dashed line) and offered by previous studies with CALIPSO (different colors of dotted lines represent different aerosol types).

Atmos. Meas. Tech. Discuss., doi:10.5194/amt-2016-390, 2017
Manuscript under review for journal Atmos. Meas. Tech.
Published: 6 February 2017

Atmospheric Measurement Techniques Discussions

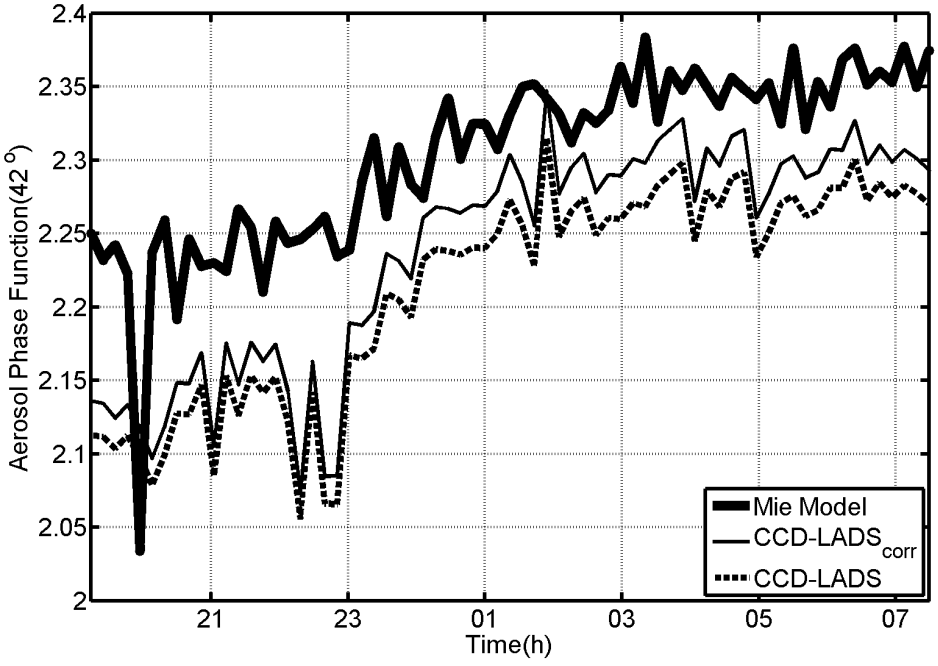

Figure 5: Comparison between aerosol phase function at 42 °scattering angle obtained from CCD-LADS measurements (the results estimated with the retrieval algorithm are shown with fine solid line, while the values estimated directly with the measurements are shown with dashed line) and modelled with modified Mie model (shown with bold solid line).

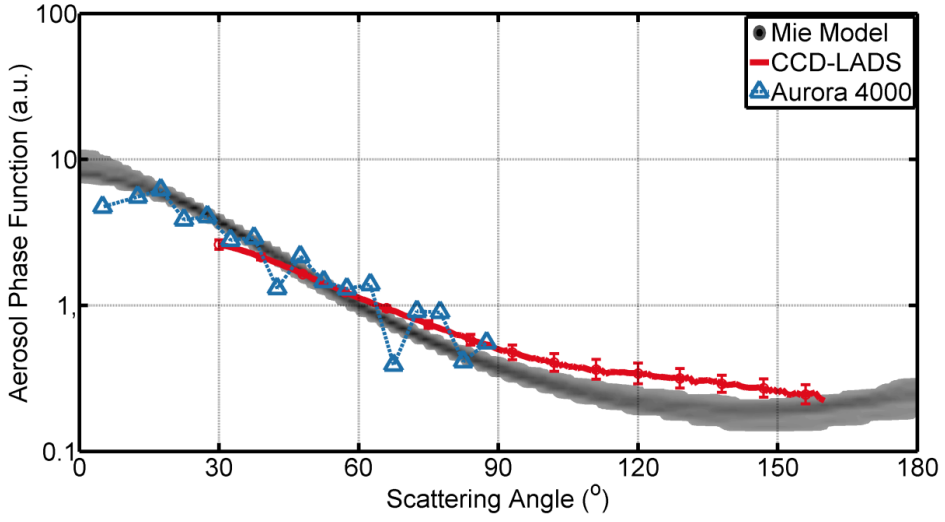

Figure 6: Comparison between aerosol phase function retrieved from CCD-LADS measurements (red line shows the average value, the error bar shows the standard deviation), measured from Aurora 4000 polar nephelometer (blue triangle) and modelled with modified Mie model (grayscale map).